Structural Basis for the Structure−Activity Relationships of Peroxisome Proliferator-Activated Receptor Agonists

Neeraj Mahindroo,[†] Yi-Hui Peng,[†,‡] Chia-Hui Lin,[§] Uan-Kang Tan,[||] Ekambaranellore Prakash,[†] Tzu-Wen Lien,[†] I-Lin Lu,[†,⊥] Hong-Jen Lee,[†] John Tsu-An Hsu,[†,#] Xin Chen,[†] Chun-Chen Liao,[§] Ping-Chiang Lyu,[‡] Yu-Sheng Chao,[†] Su-Ying Wu,*[,†] and Hsing-Pang Hsieh*[,†]

Division of Biotechnology and Pharmaceutical Research, National Health Research Institutes, 35, Keyan Road, Zhunan Town, Miaoli County 350, Taiwan, Republic of China, Department of Chemistry, Department of Life Sciences, and Department of Chemical Engineering, National Tsing Hua University, Hsinchu 300, Taiwan, Republic of China, Graduate Institute of Life Sciences, National Defense Medical Center, Taipei 114, Taiwan, Republic of China, and Department of Chemical Engineering, Northern Taiwan Institute of Science and Technology, Taipei 112, Taiwan, Republic of China

Received June 2, 2006

Type 2 diabetes has rapidly reached an epidemic proportion becoming a major threat to global public health. PPAR agonists have emerged as a leading class of oral antidiabetic drugs. We report a structure biology analysis of novel indole-based PPAR agonists to explain the structure−activity relationships and present a critical analysis of reasons for change in selectivity with change in the orientation of the same scaffolds. The results would be helpful in designing novel PPAR agonists.

Introduction

Type 2 diabetes has rapidly reached an epidemic proportion, becoming a major threat to global public health.[1] The ligands targeting peroxisome proliferator-activated receptor α/γ (PPARα/γ) or PPAR$\alpha/\gamma/\delta$ have shown promise in preclinical and clinical development, although some of these candidates were withdrawn due to adverse safety profiles.[2−4] The efforts to develop a safe and effective dual PPARα/γ agonist are continuing in view of the greater benefits offered by this class of compounds.

We have recently reported a series of indole based PPAR pan agonists with the lead compound **1** (Figure 1) displaying potent glucose lowering efficacy and an excellent pharmacokinetic profile[5] and **2** showing potent in vitro binding and functional activities.[6] We had also reported the cocrystal structures of **1** and **2** to analyze the interactions with the PPARγ protein. Here we present the effect of moving the acidic head moiety from the N1 position to the hydroxyl group of 4-, 5-, or 6-hydroxyindole and the tail part attached through a linker to the N1-positon of indole to determine the effect of this switch on the activity and selectivity with the aid of structural biology studies. This is the first report of detailed structural analysis of the PPAR agonists to explain the structure−activity relationships. The synthesis of novel indoleoxyacetic acids is also reported.

Chemistry. Compounds **7**−**12** were synthesized as shown in Scheme 1. The commercially available 4, 5, or 6-hydroxyindoles (**3a**−**c**) were alkylated with ethyl 2-bromoacetate or ethyl 2-bromo-2-methylpropionate in the presence of an equimolar amount of potassium hydroxide in DMSO yielding **4a**−**f**. Compounds **4a**−**f** were alkylated with 1-bromo-3-chloropropane under similar conditions as the previous step to give **5a**−**f**, which were then coupled with 6-hydroxy-5-propyl-2-benzoylnaphtha-

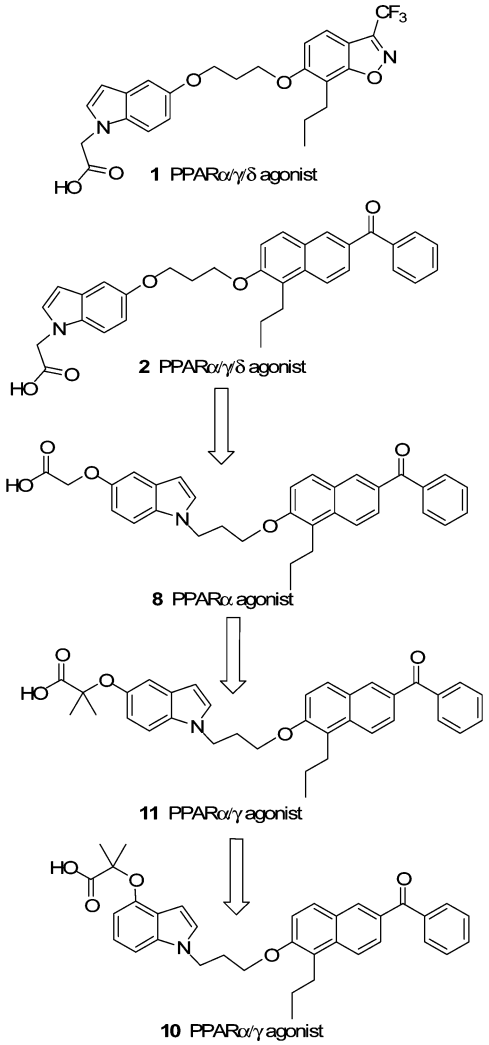

Figure 1. Transformation from PPAR-pan agonist to PPARα agonist to PPARα/γ dual agonist.

* To whom correspondence should be addressed. Tel.: 886-37-246-166 ext. 35713 (S.-Y.W.); 886-37-246-166 ext. 35708 (H.-P.H.). Fax: 886-37-586-456 (S.-Y.W.); 886-37-586-456 (H.-P.H.). E-mail: suying@nhri.org.tw (S.-Y.W.); hphsieh@nhri.org.tw (H.-P.H.).

[†] National Health Research Institutes.

[‡] Department of Life Sciences, National Tsing Hua University.

[§] Department of Chemistry, National Tsing Hua University.

[||] Department of Chemical Engineering, Northern Taiwan Institute of Science and Technology.

[⊥] Graduate Institute of Life Sciences, National Defense Medical Center.

[#] Department of Chemical Engineering, National Tsing Hua University.

10.1021/jm060663c CCC: $33.50
Published on Web 09/15/2006

Scheme 1. Synthetic Route to **7**−**12**[a]

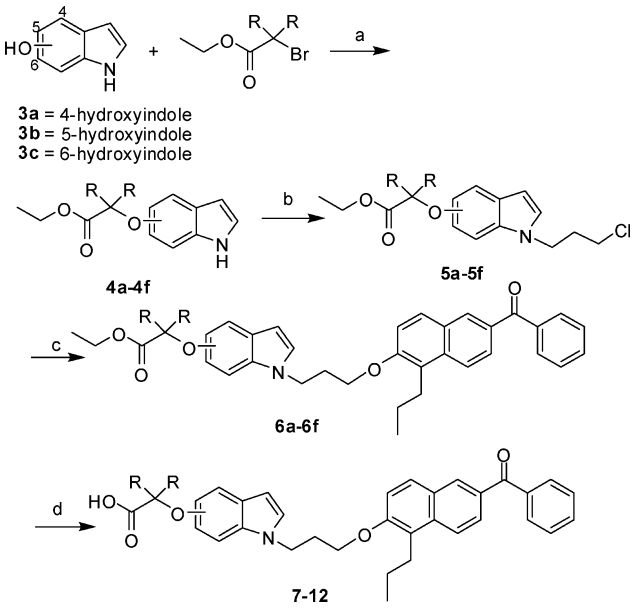

[a] Reagents: (a) KOH, DMSO, rt; (b) 1-bromo-3-chloropropane, KOH, DMSO, rt; (c) 6-hydroxy-5-propyl-2-benzoylnaphthalene, K_2CO_3, KI, DMF, 110 °C; (d) LiOH, MeOH, H_2O.

Table 1. In Vitro Human PPAR Activities of Indolyloxyalkanoic Acids

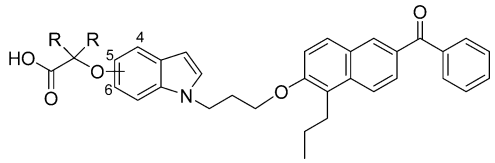

compd	R	indole position	TA EC_{50}[a,b] (μM) α	γ	δ
7	H	4	0.206	4.220	>10
8	H	5	0.032	2.210	>10
9	H	6	2.078	3.470	6.980
10	CH_3	4	0.282	0.210	4.300
11	CH_3	5	0.123	0.650	>10
12	CH_3	6	1.099	0.470	4.630
rosiglitazone				0.220	
2			0.008	0.070	0.500

[a] Concentration of test compound that produced 50% of the maximal reporter activity. [b] All data within ±15% (n = 3).

lene[6] in the presence of potassium carbonate and potassium iodide in DMF to give **6a**−**f**. Finally, **6a**−**f** were deprotected by refluxing with lithium hydroxide in a methanol−water mixture to give the desired compounds **7**−**12**.

Results and Discussion

The recently reported N1-substituted indole **2** showed potent activity against all three PPAR subtypes in binding and functional assays.[6] To take advantage of the versatility of the indole scaffold, we moved the acidic headgroup to the hydroxyl group of 4, 5, or 6-hydroxyindoles, respectively, and the hydrophobic tail part was attached through a linker to the N1 position, thus effectively reversing the placement of substituents on indole as compared to **2**. The compounds were screened in a cell-based transactivation assay[5] for all three PPAR isoforms, as shown in Table 1. Upon placing the oxyacetic acid at the 5-position of the indole, compound **8** loses PPARγ and PPARδ functional activity but retains potent PPARα activity. The 4-position analogue, **7**, also showed selective PPARα activity, while the 6-position analogue, **9**, had weak functional activity against all three subtypes. Keeping in mind the selective PPARα activity of fibrates,[7] we decided to introduce the dimethyl group on the oxyacetic acid in **7**−**9**, to synthesize the fibrates **10**−**12**, expecting to increase the PPARα activity and improve the selectivity. But to our surprise, the introduction of the fibrate moiety instead improved the PPARγ binding and functional activity of all three analogues, thus resulting in dual PPARα/γ agonists. The 5-substituted indole analogue **11** showed potent PPARα and PPARγ functional activities. On moving the acidic head to the 4-position of the indole in compound **10**, the PPARγ activity improved 3-fold and it retained potent PPARα functional activity. Additionally, the 6-substituted analogue, **12**, exhibited reversal of the relative PPARα/γ functional activity, showing 2-fold better potency for PPARγ as compared to PPARα. All the compounds showed weak or no PPARδ activity.

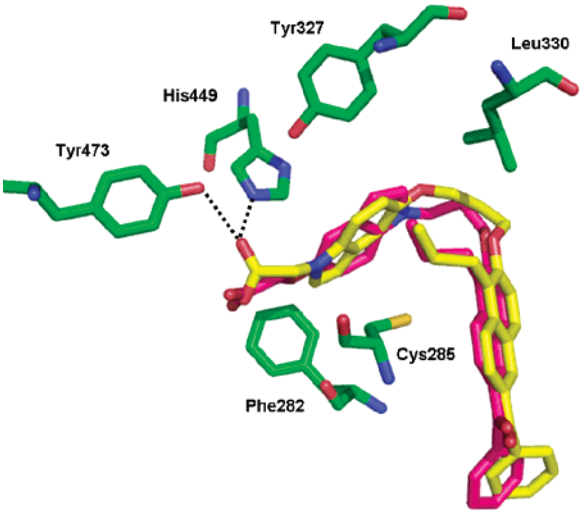

Figure 2. Comparison of cocrystal structures of **2** (yellow) and **8** (magenta) in complex with PPARγ protein (green).

The change in selectivity and relative decrease in activity on reversing the position of the acidic head and hydrophobic tail on indole scaffold in comparison to **2** induced us to carry out a detailed structural biology study of the cocrystals of compounds **2**, **8**, and **10** with PPARγ (Table 2). This would help to study the interactions of the ligand with the protein and also reveal the unusual role of the fibrate moiety in increasing the PPARγ activity, as compared to other published fibrate analogues, and thus aid in the design of novel PPAR agonists.

Superimposition of the cocrystallized structures of **2** and **8** with PPARγ revealed the difference in their binding positions (Figure 2). The tail part of these two ligands superimposed reasonably well, whereas the linker and the head parts occupied different binding positions. In the **2**−PPARγ complex structure, the longer linker allowed the indole ring to move close to the AF2 helix and, consequently, enabled the carboxylic head of **2** to form H-bond interactions with His449 and Tyr473. This H-bonding pattern was conserved in most full PPARγ agonist complex structures and, in some cases, an additional H-bond was formed with His323 or Ser289. Many reports have suggested the interactions with this conserved H-bonding rich area are important for the activities of PPARγ agonists as this H-bonding network could stabilize the AF-2 helix in a conformation favoring the binding of coactivators to PPARγ and, consequently, enhancing their recruitment.[8,9] In contrast, in the **8**−PPARγ complex structure, with a linker one oxygen length shorter, the indole ring was moved away from the AF2 helix

Table 2. Crystallographic Data and Refinement Characteristics

parameter	2	8	10
resolution (Å)	20 − 2.07	30 − 1.97	30 − 2.34
unit cell $P2_1(\alpha = \gamma = 90°)$	$a = 55.967$	$a = 56.015$	$a = 56.758$
	$b = 88.642$	$b = 88.671$	$b = 89.775$
	$c = 57.878$	$c = 58.024$	$c = 58.773$
	$\beta = 90.014°$	$\beta = 90.240°$	$\beta = 90.320°$
total reflections obsd	545 806	309 586	459 279
unique reflections	33 504	40 346	25 155
multiplicity	16.29	7.67	18.26
R_{merge} % (outer shell)	4.6 (31.3)	4.2 (28.2)	6.1 (34.9)
$\langle I/\sigma(I)\rangle$ (outer shell)	34.2 (3.41)	29.25 (4.7)	18.83 (3.95)
completeness %	97.4	99.0	99.3
(outer shell)	(98.7)	(95.8)	(100.0)
R_{work} %	21.85	23.91	23.27
R_{free} %	28.83	26.46	31.55
RMS[a] bonds (Å)	0.021	0.008	0.021
RMS[a] angles (deg)	1.919	1.300	1.891

[a] RMS = root-mean-square deviation.

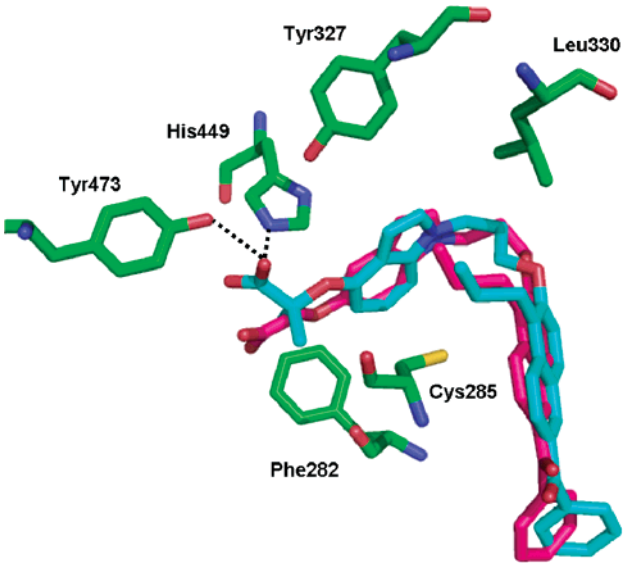

Figure 3. Comparison of cocrystal structures of **8** (magenta) and **10** (light blue) in complex with PPARγ protein (green). For clarity, the H-bonding interactions of **10** with Ser289 and His323 were omitted from the figure.

and subsequently resulted in the loss of H-bond interactions with PPARγ. The absence of these critical H-bonding interactions with the protein might provide the structural basis for the much weaker transactivation activity of **8** for PPARγ as compared with **2**.

Further, to elucidate the mechanism of the increase in PPARγ activity upon the introduction of the fibrate moiety, we carried out a structural biology study of **10**. The complex structure of **10** with PPARγ was solved to 2.34 Å, and the electron density map of the compound is very defined. Comparison of the structures of **8** and **10** showed that the indole ring, linker, and tail parts superimposed very well with each other (Figure 3). However, a most significant difference occurred in the head part, particularly around the carboxylic acid. The dimethyl group in the fibrate moiety formed hydrophobic interactions with Phe282, Cys285, and Gln286 and shifted the carboxylic acid group closer to the AF-2 helix. The movement of the carboxylic acid group led to the formation of four strong H-bonding interactions with Ser289, His323, His449, and Tyr473. Therefore, introduction of the dimethyl group was able to reposition the carboxylic acid to the area where it could form the conserved H-bonding interactions with the key residues and, consequently, increase its activity toward PPARγ.

Table 3. Distances between the Oxygens in the Acidic Head and Oxygen/Carbon in the Linker of PPAR Agonists and Protein−Ligand Intermolecular Energy, as Calculated by Insight II

compound	Ph-O to COOH or COOH to C next to N1 position of indole(Å)	PPARγ EC50 (μM)	Protein-Ligand intermolecular energy (kcal/mol)
2 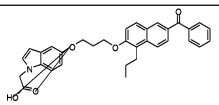	7.9 8.7	0.070	-57.49
8 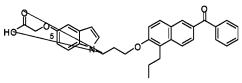	9.21 9.70	2.210	-15.29
10 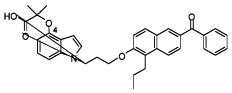	8.39 9.17	0.210	-47.96

In our recent report[6] we had shown that the distances between the acidic group and the linker, when a ligand is complexed with the PPARγ protein, were important for potent activity. We have now determined with the compounds described herein that a similar correlation exists for the distances between the carboxylic acid group and the methylene adjacent to the indole N1. As in our previous report, a distance close to 8−9 Å translated into potent PPARγ activity. Distances longer than 9 Å, as in the case of compound **8**, did not allow the molecule to orient properly in the PPARγ binding pocket, thus limiting the interactions with the narrow acidic pocket of the LBD (Table 3).

Conclusion

In conclusion, the structure−activity relationship studies revealed that 5-substituted indoleoxyacetic acid analogue **8** is a potent and selective PPARα agonist. Incorporation of the dimethyl to form fibrate analogues unexpectedly increased the PPARγ activity, giving PPARα/γ dual agonists, with the 4-substituted indole analogue **10** being most potent. The change in potency and selectivity from PPAR pan agonist (**2**), to PPARα agonist (**8**), to PPARα/γ agonist (**10**) was noted upon reversal of the orientation of the indole moiety in the indole-based PPAR agonists. The structural biology studies of the cocrystals of **2**, **8**, and **10** with PPARγ-LBD showed that the H-bond interactions of the carboxylic acid groups with the AF-2 helix were the structural basis for the PPARγ agonist activity. The repositioning of the carboxylic acid of **10** into the AF-2 helix due to the dimethyl group resulted in four H-bond interactions with key residues contributing to PPARγ agonist activity. The proper orientation of the acidic head into the AF-2 helix can be indicated by the distance between the carboxylic group and the linker and should be around 8−9 Å for potent activity.

Experimental Section

Ethyl 2-(1*H*-Indol-5-yloxy)-2-methylpropionate (4e). A mixture of 5-hydroxyindole (**3b**; 0.500 g, 3.76 mmol), powdered potassium hydroxide (0.316 g, 5.64 mmol), and DMSO (10 mL) was stirred at room temperature for 10 min, and then ethyl-2-bromoisobutyrate (0.806 g, 4.14 mmol) was added. Stirred at room temperature for 1.5 h and then 15 mL of water was added. The mixture was extracted with ethyl acetate (2 × 30 mL). The combined organic layer was washed with water (6 × 25 mL), followed by brine (2 × 20 mL), and dried over anhydrous Na_2SO_4. The solvent was removed in vacuo, and the residue flash chromatographed over silica gel, eluting with hexane/ethyl acetate (95:5) to give **4e** (0.696 g, 75%). ^{1}H NMR (300 MHz, $CDCl_3$) δ 1.28 (t, J = 7.2 Hz, 3H), 1.57 (s, 6H), 4.27 (quartet, J = 7.2 Hz, 2H), 6.42−6.43 (m, 1H), 6.84 (dd, J = 2.4, 8.4 Hz, 1H), 7.12−

7.15 (m, 2H), 7.20 (d, J = 8.7 Hz, 1H), 8.35 (br s, 1H); MS (ESI, m/z) 248.2 $(M + H)^+$.

Compounds **4a**−**d** and **4f** were prepared in a similar manner starting from the corresponding **3a**−**c**.

Ethyl 2-[1-(3-Chloropropyl)-1*H*-indol-5-yloxy]-2-methylpropionate (5e). A mixture of **4e** (0.495 g, 2.0 mmol), powdered potassium hydroxide (0.168 g, 3.01 mmol), and DMSO (10 mL) was stirred at room temperature for 10 min and then 1-bromo-3-chloropropane (0.944 g, 6.01 mmol) was added. Stirred at room temperature for 1.5 h and then added 25 mL of water. The mixture was extracted with ethyl acetate (3 × 30 mL). The combined organic layer was washed with water (6 × 25 mL), followed by brine (2 × 20 mL), and dried over anhydrous Na_2SO_4. The solvent was removed in vacuo, and the residue was flash chromatographed over silica gel, eluting with hexane/ethyl acetate (95:5) to give **5e** (0.570 g, 88%). ^{1}H NMR (300 MHz, $CDCl_3$) δ 1.30 (t, J = 7.2 Hz, 3H), 1.57 (s, 6H), 2.25 (quintet, J = 6.0 Hz, 2H), 3.46 (t, J = 6.0 Hz, 2H), 4.23−4.31 (m, 4H), 6.39 (d, J = 3.0 Hz, 2H), 6.87 (dd, J = 2.4, 8.7 Hz, 1H), 7.09−7.12 (m, 2H), 7.21 (d, J = 8.7 Hz, 1H); MS (ESI, m/z) 324.2 $(M + H)^+$.

Compounds **5a**−**d** and **5f** were prepared in a similar manner starting from corresponding **4a**−**d** and **4f**.

Ethyl 2-{1-[3-(6-Benzoyl-1-propylnaphthalen-2-yloxy)propyl]-1*H*-indol-5-yloxy}-2-methylpropionate (6e). A mixture of **5e** (0.350 g, 1.08 mmol), 6-hydroxy-5-propyl-2-benzoylnaphthalene[6] (0.314 g, 1.08 mmol), potassium carbonate (0.224 g, 0.1.63 mmol), and potassium iodide (0.036 g, 0.10 mmol) in 7 mL of DMF was heated at 110 °C for 2 h. The mixture was cooled to room temperature and quenched with water (10 mL). The mixture was extracted with ethyl acetate (3 × 20 mL). The combined organic layer was washed with water (6 × 20 mL), followed by brine (2 × 20 mL), and then dried over anhydrous sodium sulfate. The solvent was removed in vacuo, and the residue was filtered through a short silica column, eluting with hexane/dichloromethane (50:50) to give compound **5e** (0.543 g, 87%). ^{1}H NMR (300 MHz, $CDCl_3$) δ 1.10 (t, J = 7.2 Hz, 3H), 1.29 (t, J = 7.2 Hz, 3H), 1.57 (s, 6H), 1.70−1.85 (m, 2H), 2.36 (quintet, J = 6.0 Hz, 2H), 3.17 (t, J = 7.8 Hz, 2H), 4.05 (t, J = 6.6 Hz, 2H), 4.26 (quartet, J = 7.2 Hz, 2H), 4.41 (t, J = 6.6 Hz, 2H), 6.39 (d, J = 3.0 Hz, 2H), 6.84 (dd, J = 2.4, 9.0 Hz, 1H), 7.06−7.26 (m, 4H), 7.49−7.54 (m, 2H), 7.59−7.63 (m, 1H), 7.76 (d, J = 9.0 Hz, 1H), 7.86 (d, J = 8.7 Hz, 2H), 7.97 (dd, J = 1.5, 9.0 Hz, 1H), 8.07 (d, J = 9.0 Hz, 1H), 8.22 (d, J = 1.5 Hz, 1H). MS (ESI, m/z) 578.5 $(M + H)^+$.

Compounds **6a**−**d** and **6f** were synthesized in similar manner starting from appropriate starting material selected from **5a**−**d** and **5f**.

2-{1-[3-(6-Benzoyl-1-propylnaphthalen-2-yloxy)propyl]-1*H*-indol-5-yloxy}-2-methylpropionic Acid (11). The mixture of compound **6e** (0.543 g, 0.941 mmol) and LiOH (0.090 g, 3.764 mmol) in a methanol and water mixture (4:1) was refluxed for 2 h. The solvent was removed in vacuo and 0.5 N HCl was added to the residue and extracted with ether (3 × 20 mL). The combined organic layer was washed with water (2 × 20 mL), followed by brine (2 × 10 mL). The solvent was removed in vacuo, and the residue was chromatographed over a short column of silica gel, eluting with dichloromethane/methanol (98:2) to give **11** (0.465 g, 90%). ^{1}H NMR (300 MHz, $CDCl_3$) δ 1.11 (t, J = 7.5 Hz, 3H), 1.56 (s, 6H), 1.72−1.79 (m, 2H), 2.37 (quintet, J = 6.0 Hz, 2H), 3.17 (t, J = 7.8 Hz, 2H), 4.07 (t, J = 6.0 Hz, 2H), 4.43 (t, J = 6.0 Hz, 2H), 6.44 (d, J = 3.0 Hz, 1H), 6.85 (dd, J = 2.4, 9.0 Hz, 1H), 7.12 (d, J = 2.7 Hz, 1H), 7.18 (d, J = 9.0 Hz, 1H), 7.24 (d, J = 2.1 Hz, 1H), 7.261 (d, J = 9.0 Hz, 1H), 7.48−7.54 (m, 2H), 7.58−7.64 (m, 1H), 7.75 (d, J = 9.0 Hz, 1H), 7.84−7.87 (m, 2H), 7.97 (dd, J = 1.8, 9.0 Hz, 1H), 8.07 (d, J = 9.0 Hz, 1H), 8.22 (d, J = 1.5 Hz, 1H). HRMS (EI^+, m/z) calcd for $C_{35}H_{35}O_5N$, 549.2515; found, 549.2499.

Compounds **7**−**10** and **12** were synthesized in similar manner as **11** starting from **6a**−**d** and **6f**, respectively.

Acknowledgment. The authors thank Ms. Hsiao-Wen Edith Chu, Ms. Huai-Tzu Chang, Ms. Pey-Yea Yang, and Ms. Hsiu-Hsiu Huang for their administrative support, the staff at the beamline NSRRC BL13B1 and BL13C1 for technical assistance, National Health Research Institutes, Taiwan, and National Science Council of the Republic of China (Grant Nos. NSC 94-2323-B-007-001) for financial support.

Supporting Information Available: The ^{1}H NMR, HRMS, and HPLC purity data for compounds **7**−**12**, experimental procedures for transactivation assay, and structural biology studies. The coordinates and structure factors of PPARγ/compound **8** and PPARγ/compound **10** have been deposited in the Protein Data Bank with accession codes 2HWQ and 2HWR. This material is available free of charge via the Internet at http://pubs.acs.org.

References

(1) Kargul, J.; Laurent, G. J. Diabetes: New Challenges for the Control of Disease Globalisation. *Int. J. Biochem. Cell Biol.* **2006**, *38*, 685−686.

(2) Lebovitz, H. Diabetes: Assessing the Pipeline. *Atheroscler. Suppl.* **2006**, *7*, 43−49.

(3) Miller, A. R.; Etgen, G. J. Novel Peroxisome Proliferator-Activated Receptor Ligands for Type 2 Diabetes and the Metabolic Syndrome. *Expert Opin. Invest. Drugs* **2003**, *12*, 1489−1500.

(4) Staels, B.; Fruchart, J. C. Therapeutic Roles of Peroxisome Proliferator-Activated Receptor Agonists. *Diabetes* **2005**, *54*, 2460−2470.

(5) Mahindroo, N.; Huang, C. F.; Peng, Y. H.; Wang, C. C.; Liao, C. C.; Lien, T. W.; Chittimalla, S. K.; Huang, W. J.; Chai, C. H.; Prakash, E.; Chen, C. P.; Hsu, T. A.; Peng, C. H.; Lu, I. L.; Lee, L. H.; Chang, Y. W.; Chen, W. C.; Chou, Y. C.; Chen, C. T.; Goparaju, C. M. V.; Chen, Y. S.; Lan, S. J.; Yu, M. C.; Chen, X.; Chao, Y. S.; Wu, S. Y.; Hsieh, H. P. Novel Indole-Based Peroxisome Proliferator-Activated Receptor Agonists: Design, SAR, Structural Biology, and Biological Activities. *J. Med. Chem.* **2005**, *48*, 8194−8208.

(6) Mahindroo, N.; Wang, C. C.; Liao, C. C.; Huang, C. F.; Lu, I. L.; Lien, T. W.; Peng, Y. H.; Huang, W. J.; Lin, Y. T.; Hsu, M. C.; Lin, C. H.; Tsai, C. H.; Hsu, J. T. A.; Chen, X.; Lyu, P. C.; Chao, Y. S.; Wu, S. Y.; Hsieh, H. P. Indol-1-yl Acetic Acids as Peroxisome Proliferator-Activated Receptor Agonists: Design, Synthesis, Structural Biology, and Molecular Docking Studies. *J. Med. Chem.* **2006**, *49*, 1212−1216.

(7) Shearer, B. G.; Hoekstra, W. J. Recent Advances in Peroxisome Proliferator-Activated Receptor Science. *Curr. Med. Chem.* **2003**, *10*, 267−280.

(8) Nolte, R. T.; Wisely, G. B.; Westin, S.; Cobb, J. E.; Lambert, M. H.; Kurokawa, R.; Rosenfeld, M. G.; Willson, T. M.; Glass, C. K.; Milburn, M. V. Ligand Binding and Co-activator Assembly of the Peroxisome Proliferator-Activated Receptor-γ. *Nature* **1998**, *395*, 137−143.

(9) Lu, I. L.; Huang, C. F.; Peng, Y. H.; Lin, Y. T.; Hsieh, H. P.; Chen, C. T.; Lien, T. W.; Lee, H. J.; Mahindroo, N.; Prakash, E.; Yueh, A.; Chen, H. Y.; Goparaju, C. M.; Chen, X.; Liao, C. C.; Chao, Y. S.; Hsu, J. T.; Wu, S. Y. Structure-Based Drug Design of a Novel Family of PPARγ Partial Agonists: Virtual Screening, X-ray Crystallography, and in Vitro/in Vivo Biological Activities. *J. Med. Chem.* **2006**, *49*, 2703−2712.

JM060663C